Available online at www.sciencedirect.com
ScienceDirect
Tetrahedron: Asymmetry
Tetrahedron: *Asymmetry* 18 (2007) 1540–1547

Sterically hindered and completely arrested nitrogen inversion in pyrazolidines☆

Sergey V. Usachev,[a] Grygorii A. Nikiforov,[b] Konstatin A. Lyssenko,[c] Yulia V. Nelubina,[c] Pavel A. Levkin[a] and Remir G. Kostyanovsky[a,*]

[a]*Semenov Institute of Chemical Physics, Russian Academy of Sciences, 4 ul. Kosygina, 119991 Moscow, Russia*
[b]*Emanuel Institute of Biochemical Physics, Russian Academy of Sciences, 4 ul. Kosygina, 119991 Moscow, Russia*
[c]*Nesmeyanov Institute of Organoelement Compounds, Russian Academy of Sciences, 28 ul. Vavilova, 119991 Moscow, Russia*

Received 9 May 2007; accepted 20 June 2007

Abstract—Syntheses of *trans*-1,2-di-*tert*-butylpyrazolidine **1**, *d,l*- and semi-*meso*-1,2-diisopropyl-3,5-dimethylpyrazolidines, **2a** and **2b**, respectively, have been developed. Activation parameters of the nitrogen inversion in **1** ($\Delta G^{\neq} = 123$ kJ mol^{-1} at 110 °C, $\Delta H^{\neq} = 114$ kJ mol^{-1}, $\Delta S^{\neq} = -15$ J K^{-1} mol^{-1}) have been determined. The steric veto of the nitrogen inversion in **2a** has been confirmed. Chemical transformations of **1** have been studied, and the crystal structures of **2a**·picrate and **2b**·HCl determined.

1. Introduction

Sterically hindered nitrogen inversion in cyclic hydrazines, a new direction of the investigation of asymmetric nitrogen, has been developed over the last decade. In tertiary amines, increasing the bulk of the substituents causes the ground state to be destabilized up to full planarization of the N-atom, corresponding to a transition state whereas in cyclic hydrazines it leads to destabilization of the transition state of inversion up to its complete veto. Four types of cyclic hydrazines I–IV (Tables 1 and 2) were synthesized and studied.

The activation parameters given in Tables 1 and 2 convincingly show that the barriers of nitrogen inversion considerably rise with an increase in the bulk of the *N*-substituents. 1,2-Di-*tert*-butylpyrazolidine **1** is so highly configurationally stable, that in the ^{13}C NMR spectrum, the signal of 3,5-C at 42 ppm (dd with $^{1}J = 10$ Hz) is not transformed into a triplet (in [$^{2}H_8$]-toluene at 100 °C). Complete resolution of (±)-**1** was detected by GLC on Chirasil-β-Dex chiral stationary phase[11] at 110 °C. The concept of a steric veto of nitrogen inversion in 1,2,3,5-tetrasubstituted pyrazolidines has already been reported,[10] and 1,2-diisopropyl-3,5-dimethylpyrazolidin was synthesized.[11]

Table 1. Nitrogen inversion barriers in cyclic hydrazines I, II and III

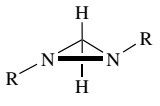 I	$\Delta G^{\neq}$/kJ mol^{-1} (T/°C)	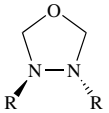 II	$\Delta G^{\neq}$/kJ mol^{-1} (T/°C)	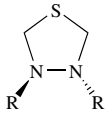 III	$\Delta G^{\neq}$/kJ mol^{-1} (T/°C)
R = *t*-Bu[2]	136 (150.7)[4]	R = *t*-Bu[5,6]	142 (170)[9]	R = *i*-Pr[6]	80 (66)[6]
R = *n*-Bu[2]	123 (115)[4]	R = *i*-Pr[7,8]	81 (111)[7,8]		
R = Ad[3]	—	R = Et[7,8]	50 (−31)[7,8]		
		R = Me[7,8]	44 (−61)[7,8]		

☆ Asymmetric Nitrogen. Part 102, for Part 101 see Ref. 1.

* Corresponding author. Tel.: +7 495 137 32 27; fax: +7 495 137 82 84; e-mail: kost@chph.ras.ru

0957-4166/$ - see front matter
doi:10.1016/j.tetasy.2007.06.022

Table 2. Nitrogen inversion barriers in pyrasolidines IV a–d

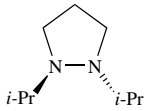	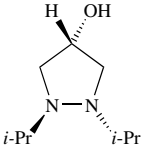	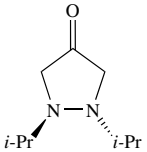	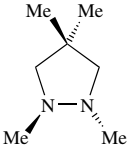
(a) $\Delta G^{\neq} = 68$ kJ mol^{-1} (25 °C)[10]	(b) $\Delta G^{\neq} = 70$ kJ mol^{-1} (25 °C)[10]	(c) $\Delta G^{\neq} = 73$ kJ mol^{-1} (25 °C)[11]	(d) $\Delta G^{\neq} = 46$ kJ mol^{-1} (−45 °C)[12,13]

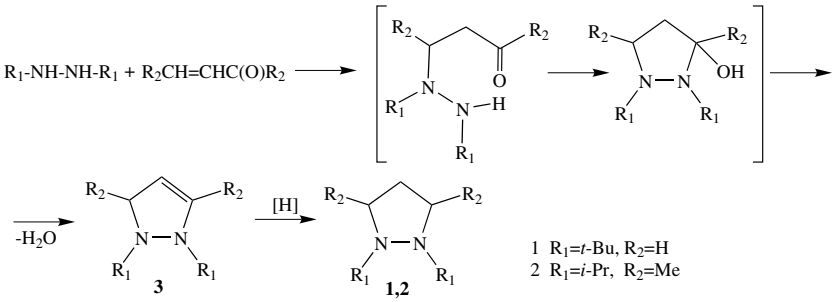

Scheme 1. The synthesis of sterically hindered pyrazolidines **1** and **2**.

2. Results and discussion

Herein we report a detailed investigation of pyrazolidines **1** and **2** synthesized as described earlier (Scheme 1).[11]

It should be noted that reaction of 1,2-di-*tert*-butylhydrazine with acrolein was carried out under more severe conditions (75–80 °C, 1 h, yield 78%), in comparison to the reaction of *N*,*N*-diisopropylhydrazine with methylpropenylketone (4–10 °C, 1 h, yield 81%).

Pyrazolines **3** are cyclic enhydrazines[14] and can undergo reactions that are typical for enamines.[15] It is known[16] that aluminium hydrides (AlH_3, $AlClH_2$ and $AlCl_2H$) in ether smoothly reduce enamines to saturated tertiary amines with high yields. This method was used for the reduction of pyrazolines **3**. However, the reduction of **3** under these conditions was found to result in formation of a mixture of **1** and **3** in a constant ratio of 1:1 (according to ^{1}H NMR spectroscopy). Fractional distillation, as well as column chromatography, on silica gel were unsuccessful to separate the mixture. Changing the reaction conditions (time, temperature, increase in concentration of the reducing agent), and repeated reduction of the produced mixture under the same conditions do not influence the ratio of the products, apparently due to formation of the stable complex of pyrazoline **3** and pyrazolidine **1** with reducing agents, which then prevents the further reduction.

Therefore, the reduction of **3** was performed by treating it with formic acid (98%), by the earlier method successfully used for hydrogenation of enamines.[17] Although the yield of **1** did not exceed 40–45%,[†] the yield of **2** reached 80%.

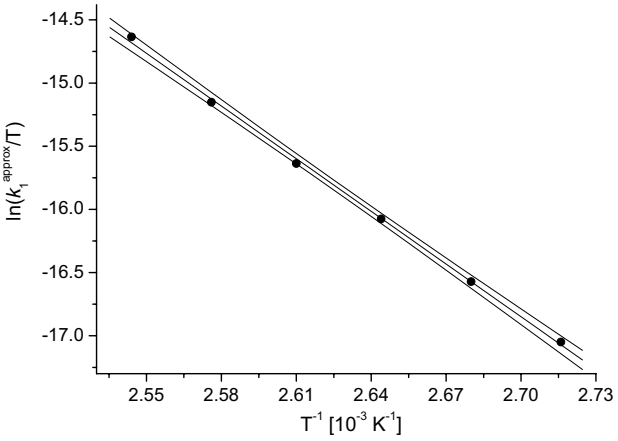

Figure 1. Eyring plot for the determination of the activation parameters $\Delta H^{\#}$ and $\Delta S^{\#}$ of 1,2-di-*tert*-butylpyrazolidine **1** from the DGC experiment. The upper and lower curves represent the error bands of the linear regression with a level of confidence of 95%. Activation parameters calculated: $\Delta H^{\#} = 114 \pm 2$ kJ mol^{-1} and $\Delta S^{\#} = -15 \pm 5$ J mol^{-1} K^{-1}.

The high configurational stability of **1** has been shown recently.[11] Herein, the activation parameters of nitrogen inversion in **1** ($\Delta H^{\neq} = 114 \pm 2$ kJ mol^{-1} and $\Delta S^{\neq} = -15 \pm 5$ J mol^{-1} K^{-1}) (Figs. 1 and 2; Table 3) were determined using dynamic gas chromatography (DGC) on chiral stationary phase (CSP), Chirasil-β-Dex.

The data given in Table 3 confirm the high configurational stability of **1**. However, the resolution of **1** into enantiomers by HPLC on microcrystalline triacetyl cellulose[‡] was not possible, and all attempts to separate the enantiomers of **1** by fractional crystallization via diastereomeric

[†] Obviously the low yield of **1** is connected with N-dealkylation under the action of formic acid (see Scheme 3).

[‡] Enantiomers of substituted diaziridines are well separated on this sorbent.[18]

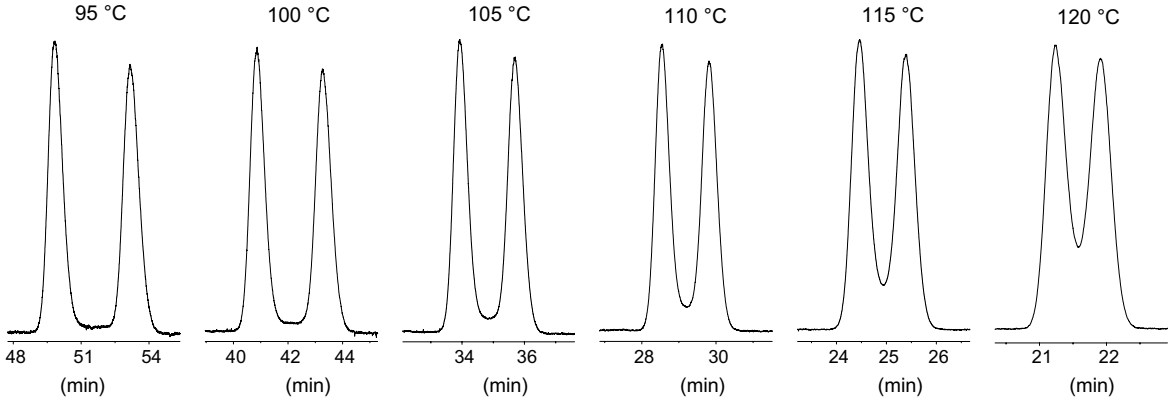

Figure 2. Chromatograms from the temperature-dependent DGC experiment for **1**. Chromatographic conditions: 25 m Chirasil-β-Dex (0.25 mm i.d., film thickness 0.25 μm). Carrier gas: dihydrogen, $P = 10$ kPa.

Table 3. The data from the DGC experiment, rate constants of the enantiomerization of **1** in the presence of CSP Chirasil-β-Dex and enantiomerization barrier of **1** at different temperatures

T [°C]	α	t_M [min]	t_1 [min]	t_2 [min]	w_1 [s]	w_2 [s]	$h_{plateau}$ [%]	k_1^{approx} [10^{-5} s^{-1}]	$\Delta G^{\#}$ [kJ mol^{-1}]
95	1.076	6.25	49.83	53.16	42.80	46.58	2.01	1.5 ± 0.2	123 ± 0.3
100	1.070	6.28	40.92	43.33	35.50	38.30	3.10	2.4 ± 0.3	123 ± 0.3
105	1.064	6.31	33.99	35.75	29.92	32.04	5.00	4.0 ± 0.5	123 ± 0.4
110	1.057	6.34	28.62	29.89	25.46	27.20	8.29	6.2 ± 0.7	123 ± 0.4
115	1.052	6.40	23.39	24.24	20.88	22.00	15.29	10.2 ± 1.2	123 ± 0.4
120	1.046	6.36	21.17	21.86	18.56	19.60	28.56	17.4 ± 2.0	123 ± 0.4

salts with (*S*)-(+)-10-camphorsulfonic acid from acetone failed.

The enantiomers of **1** were successfully separated through diastereomeric salts with (*R*)-(−)-1,1′-binaphthyl-2,2′-diyl hydrogenphosphate.[§] Unlike the ^{1}H NMR spectra of the salts with (*S*)-(+)-10-camphorsulfonic acid, in the spectra of the salts of **1** with (*R*)-(−)-1,1′-binaphthyl-2,2′-diyl hydrogenphosphate, the signals from the diastereomers were differentiated (Table 4).

The purest fraction was recrystallized from acetone to give a sample with $[\alpha]_D^{20} = -11.2$ (c 0.032, MeOH) and ee $\geqslant 93\%$ (according to ^{1}H NMR).

After treating the sample with 6 M HCl and isolating (*R*)-(−)-1,1′-binaphthyl-2,2′-diyl hydrogenphosphate, the mother liquor was evaporated under reduced pressure and the residue was treated with aqueous alkali. However, instead of the expected enantiomer of **1**, 1-*tert*-butyl-4,5-dihydro-1*H*-pyrazole **6** was obtained (yield 70%), which was transformed into crystalline tosylate **7** (Scheme 2).

An excess of strong acid apparently causes the dealkylation of salt **4**.[¶] According to ^{1}H NMR spectroscopy, the isolated compound **5** is 1-*tert*-butylpyrazolidine hydrochloride, which rapidly oxidizes into pyrazoline[††] **6** during alkalization. The structure of **7** is confirmed by ^{1}H NMR and X-ray diffraction (XRD) data.

Table 4. The influence of anion type on the NMR spectra of *t*-Bu groups in pyrazoline **1** salts

Salts of pyrazolidine **1**	δ Me_3C	Solvent
Hydrogen sulfate[11]	1.19 (br s, 9H), 1.32 (br s, 9H)	Acetone-d_6
p-Toluenesulfonate[11]	1.27 (s, 9H), 1.42 (s, 9H)	$CDCl_3$
(*S*)-(+)-10-Camphorsulfonate	1.34 (s, 9H), 1.47 (s, 9H)	$CDCl_3$
(*R*)-(−)-1,1′-Binaphthyl-2,2′-diyl hydrogenphosphate	1.16 (s, 9H), 1.28 (s, 9H), 1.30 (s, 9H), 1.38 (s, 9H)	$CDCl_3$

Pyrazolidine **2** was obtained as a mixture of (*dl*)- and semi-*meso*-forms, **2a** and **2b**, respectively (Scheme 3). Crystallization of the mixture from benzene was used to enrich **2a** up to 90–93%. The pure (*dl*)-form was separated as a picrate from a methanol solution. Structures of **2a**·picrate and **2b**·HCl were confirmed by an XRD study.

The possibility of the diastereomerization of **2a** (Fig. 3) was examined by gas chromatography on a chiral stationary phase. Only the two peaks of the analyte enantiomers were observed, that is, no diastereomers of **2** were formed under

[§] This acid is successfully used for separation of diastereomeric salts of Tröger base.[19]

[¶] In independent experiment it is shown that treatment of **1** itself with quadruple surplus of 6 M HCl in methanol leads to the same product **6**. In case of **2** such transformations was not observed.

[††] It is known, that tertiary hydrazines are quickly oxidized into corresponding hydrazones.[20]

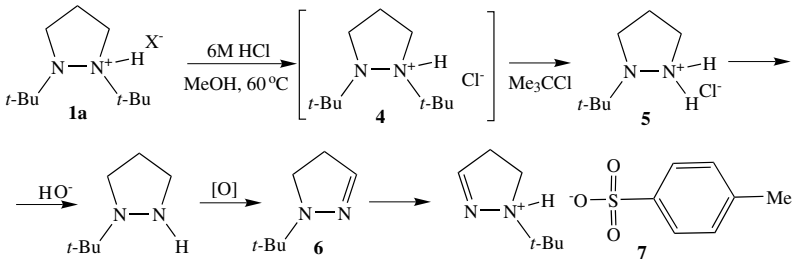

Scheme 2. The formation of 1-*tert*-butyl-4,5-dihydro-1*H*-pyrazole **6** and its crystalline tosylate **7**.

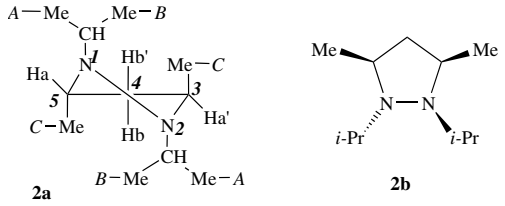

Scheme 3. (*dl*)-**2a** and semi-*meso*-**2b** forms of 1,2-diisopropyl-3,5-dimethylpyrazolidine **2**.

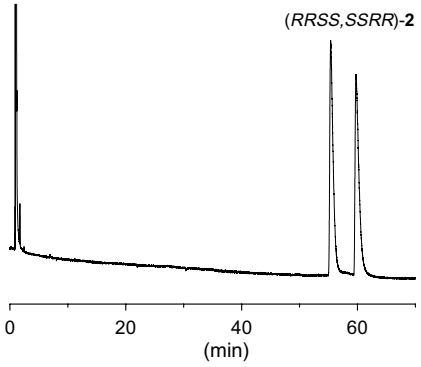

Figure 3. Chromatogram of the enantioseparation of **2** by gas chromatography. Chromatographic conditions: 20 m Chirasil-β-Dex (0.25 mm i.d., film thickness 0.25 μm). Carrier gas: dihydrogen, $P = 50$ kPa.

Table 5. Crystal data and structure refinement parameters for **2a**·picrate, **2b**·HCl and **7**

Compound	**2a**·picrate	**2b**·HCl	**7**
Empirical formula	$C_{17}H_{27}N_5O_7$	$C_{14}H_{28}ClN_2$	$C_{14}H_{22}N_2O_3S$
Formula weight	413.44	259.83	298.40
Temperature (K)	120	100	100
Crystal system	Monoclinic	Monoclinic	Monoclinic
Space group	*C*2/*c*	$P2_1/n$	$P2_1$
Z	8	4	2
a, Å	17.3903(9)	7.4082(7)	9.3378(8)
b, Å	13.9780(7)	10.2084(9)	8.8648(7)
c, Å	16.5587(9)	20.547(2)	9.5610(8)
β, °	98.785(5)	98.867(6)	112.406(6)
V, Å^3	3977.9(4)	1535.3(2)	731.69(10)
Density, g cm^{-3}	1.381	1.124	1.354
μ(Mo Kα), cm^{-1}	1.08	2.33	2.31
F(000)	1760	572	320
$2\theta_{max}$, °	56	56	58
Number of measured refl.	20,157	9840	5925
Number of independent refl. (*R*(int))	4788	3693	3569
Number of observed refl. with $I > 2\sigma(I)$	3672	2576	3254
Parameters	366	158	185
*R*1	0.0496	0.0438	0.0322
*wR*2	0.1423	0.1293	0.0784
GOF	1.019	1.003	1.001
$\Delta\rho_{max}$, $\Delta\rho_{min}$ (e Å^{-3})	0.470, −0.239	0.352, −0.226	0.331, −0.271

these conditions. Interconversion of the enantiomers, which could be detected by the appearance of a middle peak, was also not observed.

According to the X-ray diffraction study of the single crystals of **2a**·picrate, **2b**·HCl and **7** (Table 5) only one of the salts, namely, **2b**·HCl, crystallizes as a solvate with the benzene cation in a 2:1 ratio. It is noteworthy that **2a**·picrate and **2b**·HCl both crystallize in centrosymmetric space groups, while **7** is in a non-centrosymmetric chiral space group $P2_1$ is a non-resolvable conglomerate. According to the ^{1}H NMR spectra of **7** in solution, α-protons are equivalent, which indicates the fast exchange of the proton at the asymmetric nitrogen atom.

The bond lengths of pyrazolidine in **2a**·picrate and **2b**·HCl are typical for this type of heterocycles whereas in the crystal of pyrazoline **7**, there are two different N–C bonds (Table 6). The conformation of the heterocycle is an ideal envelope in **2a**·picrate and **2b**·HCl and flattened one in the case of **7** with the deviation of C(2) atom by 0.477(3) Å in **2a**·picrate (Fig. 4a) and atom C(1) by 0.540(3) and 0.139(4) Å in **2b**·HCl (Fig. 5) and **7** (Fig. 7a), respectively.

As expected the configuration of nitrogen atoms, with the exception of N(2) in the crystal of **7**, can be described as a trigonal pyramid. The deviation of the N(1) atom from the plane formed by C(1), N(2) and C(6) [C(4) in the case of **7**] varies in the range of 0.429(3)–0.484(3) Å, the corresponding parameter for the N(2) atom is 0.459(3) and 0.488(3) Å in **2b**·HCl and **2a**·picrate, respectively.

The mutual disposition of the methyl and isopropyl groups of the cation in **2a**·picrate with respect to the plane of the

Table 6. Selected bond lengths (Å) and angles (degr) of the cation in the crystals of **2a**·picrate, **2b**·HCl and **7**

Parameter	**2a**·picrate	**2b**·HCl	**7**
N(1)–N(2)	1.4759(15)	1.4716(19)	1.478(2)
N(1)–C(1)	1.5362(17)	1.525(2)	1.510(2)
C(1)–C(2)	1.521(2)	1.514(2)	1.529(2)
C(2)–C(3)	1.521(2)	1.530(2)	1.487(2)
N(2)–C(3)	1.4874(17)	1.496(2)	1.265(2)
N(2)–N(1)–C(1)	108.69(10)	106.47(13)	108.51(12)
N(1)–N(2)–C(3)	106.99(10)	107.52(13)	107.13(14)
C(1)–C(2)–C(3)	104.66(11)	103.52(14)	102.08(13)
C(1)–N(1)–C(6)[a]	112.50(10)	118.63(14)	116.63(13)
N(2)–N(1)–C(6)[a]	109.56(10)	111.40(13)	110.88(12)
N(1)–N(2)–C(9)	110.76(10)	109.84(13)	—
C(3)–N(2)–C(9)	116.06(11)	115.21(14)	—

[a] C(1)–N(1)–C(4) and N(2)–N(1)–C(4) angles in the case of **7**.

central ring is the transoid one. In contrast to **2a**·picrate, the methyl substituents of pyrazolidine in **2b**·HCl are in a cisoid conformation. The determination of the relative configuration of the asymmetric nitrogen atoms has revealed that the structure of **2a**·picrate corresponds to the (*dl*)-form of the 1,2,3,5-tetra substituted pyrazolidine while in crystalline **2b**·HCl the semi-*meso*-form is realized.

The analysis of crystal packing revealed that in racemic **2a**·picrate, **2b**·HCl and homochiral **7** crystals the cation and anion form close pairs by means of N(1)–H(1N)···O(1) (N···O is 2.817(2) Å and 2.718(3) Å, NHO angle is 173° and 177° in **2a**·picrate and **7**, respectively) (Figs. 4a and 6) or N(1)–H(1N)···Cl(1) (N···Cl is 3.022(2) Å, NHCl angle is 157°) H-bonds (Fig. 5). The close pairs are assembled by anion···anion stacking in

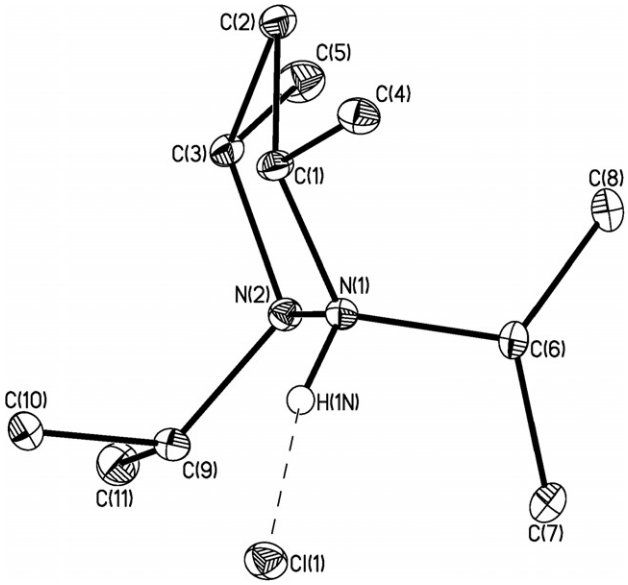

Figure 5. General view of molecule **2b**·HCl in thermal ellipsoids at the 30% probability level.

2a·picrate (Fig. 4b) and C–H···Cl weaker contacts with solvate molecule in **2b**·HCl into centrosymmetric dimers.

In all the salts studied, the above associates are held together by weak C–H···O and/or C–H···C interactions resulting in the formation of three-dimensional framework (Fig. 6). Accordingly, the type of the supramolecular organization and the chirality of a crystal are mainly governed not by strong but rather weak intermolecular interactions, as was previously observed for crystalline imidazolidine-2-one derivatives.[24]

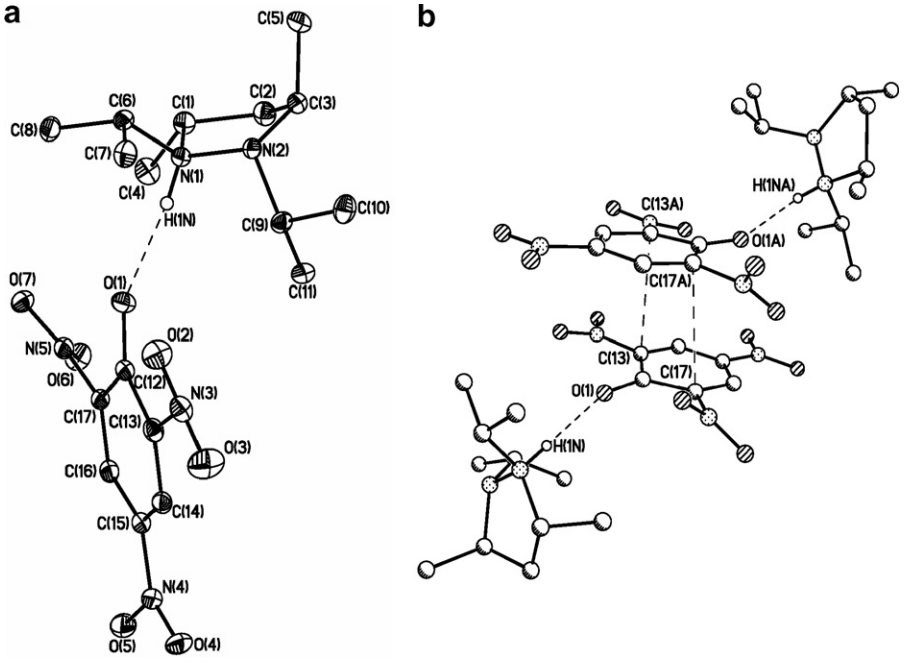

Figure 4. General view of molecule **2a**·picrate in thermal ellipsoids at the 30% probability level (a) and the stacking dimer in the crystal of **2a**·picrate (the C(13)···C(13A) and C(17)···C(17A)) distances are 3.398(3)–3.253(3) Å. (b) The atoms with label A are obtained from the basic one by symmetry operation $1 - x$, y, $0.5 - z$.

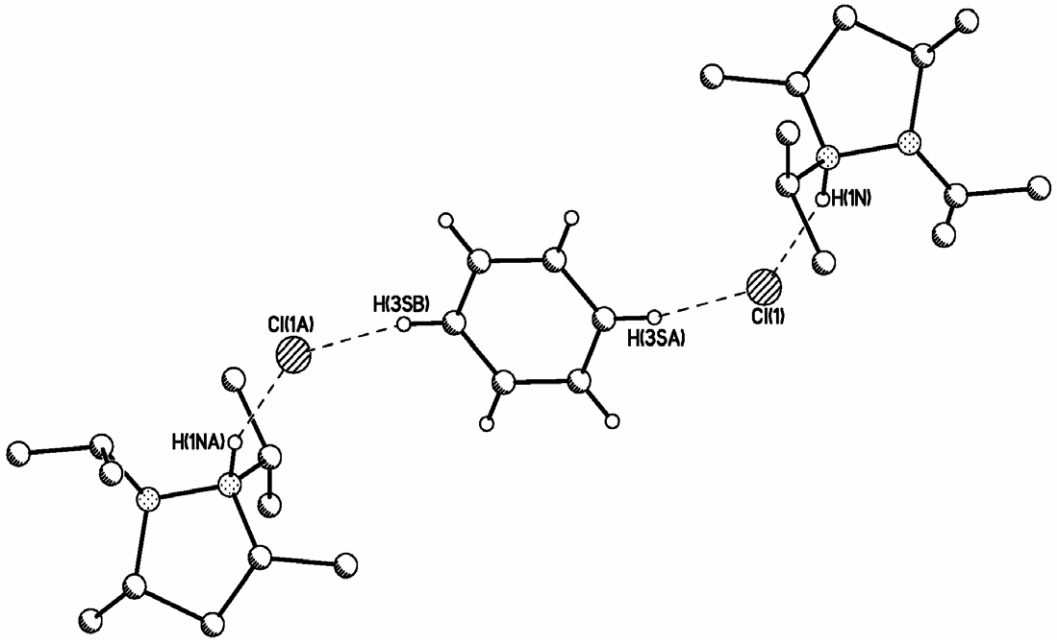

Figure 6. The N–H···Cl···H–C bonded dimer in the crystal of **2b**·HCl. The atoms with a are obtained from the basic one by symmetry operation $-x$, $-y$, $-z$.

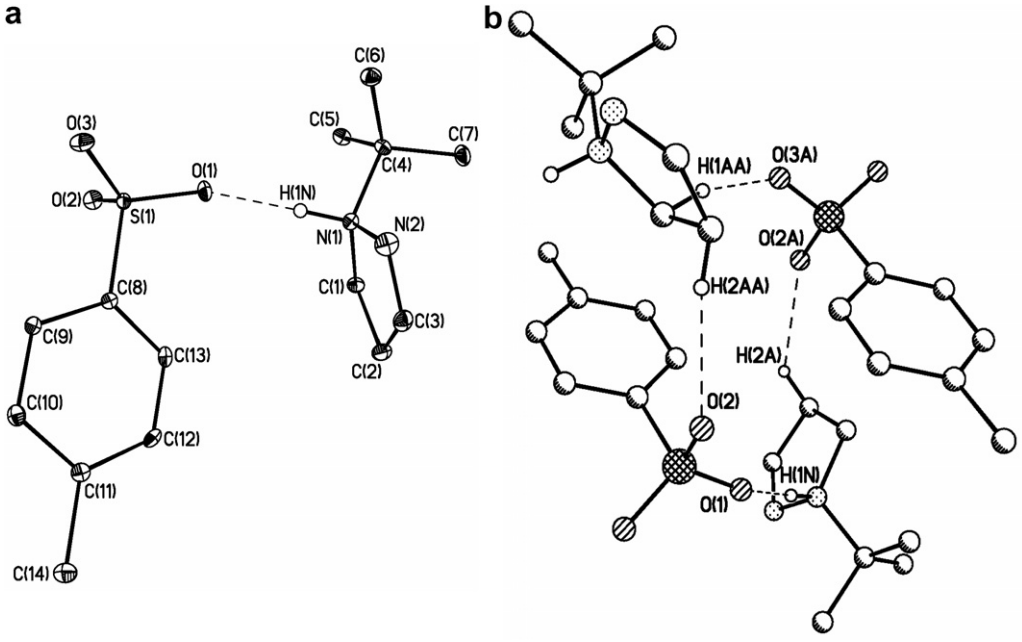

Figure 7. The general view of molecule **7** in thermal ellipsoids at the 30% probability level (a) and the fragment of three-dimensional framework in the crystal **7** (b). The atoms with A are obtained from the basic one by symmetry operation $1 - x$, $0.5 + y$, $1 - z$.

3. Conclusions

Thus, as suggested previously,[11] high configurational stability of 1,2-diisopropyl-3,5-dimethylpyrazolidin enantiomers via steric veto of the nitrogen inversion has been proved. Therefore, because of the chemical stability of the compound towards strong acids, resolution of 1,2-diisopropyl-3,5-dimethylpyrazolidin into enantiomers can be performed through diastereomeric salts.

4. Experimental

^{1}H NMR spectra were measured on spectrometers Bruker WM-400 (400.13 MHz).

S-(+)-10-Camphorsulfonate of **1**: yield 91%, mp 152–154 °C (acetone). ^{1}H NMR ($CDCl_3$) δ: (*a*-acid, *p*-pyrazolidine) 0.85[a] (s, 3H, CH_3), 1.17[a] (s, 3H, CH_3), 1.34[p] (s, 9H, Me_3CN), 1.46[p] (s, 9H, Me_3CN^+), 1.61[a] (m, 1H, CH),

Table 7. Diastereoisomeric composition (D/C), the form of crystals and its melting point

Fraction	D/C[b]	The form of crystals	Mp (°C)
Initial crystals	1/1	Fine a plate	251–254
1	2/1	Fine a plate	251–253
2	2/1	Fine a plate	—
3	1/5	Thin needles	—
4	1/13	Thin needles	258–260
5[a]	5/1	Fine a plate	249–251

[a] The fraction obtained after recrystallization of fractions 1 and 2 from acetone.

[b] The correlation of the sum of integral intensities of signal at 1.16 and 1.38 ppm to the sum of intensities of signal at 1.27 and 1.28 ppm (see Table 3).

1.83[a] (m, 2H, CH_2), 2.01[a] (m, 2H, CH_2): CH_2^p: 2.17 (m, 1H), 2.81 (m, 1H), 3.17 (m, 1H), 3.56 (m, 2H), 4.23 (m, 1H); CH_2CO: 2.29 (t, 1H), 2.34 (t, 1H); CH_2SO_3: 2.83[a] (d, 1H), 3.35[a] (d, 1H).

Fractional crystallization of the diastereomeric salt of **1** with (*R*)-(−)-1,1′-binaphthyl-2,2′-diyl hydrogenphosphate from a mixture of acetone/dichloromethane (1/1 vol.) led to five crystal fractions of different morphology, melting point and diastereomeric composition. The relative intensity of the signals of diastereomers varied depending on the fraction of crystals and their form (Table 7).

R-(−)-1,1′-Binaphthyl-2,2′-diyl hydrogenphosphonate of **1**: yield 89%, mp 251–254 °C (acetone). ^{1}H NMR ($CDCl_3$) δ: 1.16 (s, 9H, Me_3C), 1.28 (s, 9H, Me_3C), 1.30 (s, 9H, Me_3C), 1.38 (s, 9H, Me_3C); CH_2: 2.06 (m, 1H), 2.19 (m, 1H), 3.05 (m, 1H), 3.45 (m, 2H), 3.95 (m, 1H); CH_{Ar}: 7.20 (t, 2H), 7.37 (t, 4H), 7.51 (d, 2H), 7.88 (dt, 4H); 11.77 (s, 1H, HN^+).

1-tert-Butyl-4,5-dihydro-1H-pyrazole **6**: A solution of **1a** in methanol was acidified with a fourfolded excess of 6 M HCl. 1,1-Binaphtylposphonic acid was separated, and the mother liquid evaporated in vacuo. The residue, **5·HCl**, was dissolved in water, filtered and basified. The base was extracted with CH_2Cl_2. Yield **6** 70%. ^{1}H NMR ($CDCl_3$) δ: 1.15 (s, 9H, Me_3C); 2.62 (dt, 2H, $^3J = 9.6$ Hz, $^3J = 1.7$ Hz); 3.01 (t, 2H, CH_2N, $^3J = 9.6$ Hz); 6.75 (t, 1H, HCN, $^3J = 1.7$ Hz).

5·HCl: ^{1}H NMR ($CDCl_3$) δ: 1.36 (s, 9H, Me_3C); 2.24 (q, 2H, CH_2); 3.19 (br t, 2H, NCH_2); 3.19 (br t, 2H, CH_2N); 3.35 (br t, 2H, CH_2N^+).

p-Toluenesulfonate **7**: ^{1}H NMR ($CDCl_3$) δ: 1.42 (s, 9H, Me_3C); 2.43 (s, 3H, CH_3); 3.35 (br m, 2H, CH_2); 4.15 (br m, 2H, NCH_2); 7.15 (d, 2H, H_{Ph}), 7.22 (d, 2H, H_{Ph}); 7.94 (s, 1H, NCH).

Picrate **2a**: mp 118–119 °C (methanol). ^{1}H NMR ($CDCl_3$) δ: 1.16 (d, 3H, A-*Me*CHN-1, $^3J = 6.5$ Hz); 1.20 (d, 3H, C-*Me*CHN-1, $^3J = 7.08$ Hz); 1.23 (d, 3H, B-*Me*CHN-1, $^3J = 6.5$ Hz); 1.38 (d, 3H, C-*Me*CHN$^+$-2, $^3J = 6.6$ Hz); 1.42 (d, 3H, B-*Me*CHN$^+$-2, $^3J = 6.6$ Hz); 1.60 (d, 3H, C-*Me*CHN$^+$-2, $^3J = 6.87$ Hz); 2.01 (dt, 1H, Hb, $^2J = -12.7$ Hz, $^3J_{HbHa} = {}^3J_{HbHa'} = 7.8$ Hz); 2.08 (ddd, 1H, Hb′, $^2J = -12.7$ Hz, $^3J_{Hb'Ha} = 4.59$ Hz, $^3J_{Hb'Ha'} = 1.83$ Hz); 3.73 (sept, 1H, HCN-1, $^3J = 6.5$ Hz); 3.75 (sept, 1H, HCN$^+$-2, $^3J = 6.6$ Hz), 3.81 (ddq, 1H, Ha, $^3J_{HaHb'} = 4.59$ Hz, $^3J_{HbHa} = 7.8$ Hz); 8.85 (ddq, 1H, Ha′, $^3J_{Ha'Hb'} = 1.83$ Hz, $^3J_{HbHa'} = 7.8$ Hz); 8.82 (s, 2H, H_{Ar}); 10.04 (s, 1H, HN^+).

X-ray diffraction experiments were carried out with a Bruker SMART 1000 CCD diffractometer [λ(Mo Kα) = 0.71072 Å, ω-scans, $2\theta < 56°$] at 120 K for **2a**·picrate and with a Bruker SMART APEX2 CCD diffractometer [λ(Mo Kα) = 0.71072 Å, ω-scans] at 100 K for **2b**·HCl and **7**. Low temperature of the crystals was maintained with a Cryostream (Oxford Cryosystems) open-flow N_2 gas cryostat. Reflection intensities were integrated using SAINT software and absorption correction was applied semi-empirically using SADABS program. The structure was solved by direct method and refined by the full-matrix least-squares technique against F^2 in the anisotropic–isotropic approximation. All hydrogen atoms of **2a**·picrate were located from the Fourier synthesis of the electron density and refined in the isotropic approximation. In the case of **2b**·HCl and **7** only hydrogen atoms of NH groups were located from the Fourier synthesis of the electron density and refined in the isotropic approximation. The H(C) atom positions were calculated. The hydrogen atoms H(C) were refined in the isotropic approximation in the riding model. Crystal data and structure refinement parameters for **2a**·picrate, **2b**·HCl and **7** are given in Table 6. All calculations were performed using the SHELXTL software (Sheldrick, G. M. SHELXTL-97, Version 5.10, Bruker AXS Inc., Madison, WI 53719, USA).

The racemate of **2a** was enantioseparated by gas chromatography on a chiral stationary phase (CSP) Chirasil-β-Dex[21,22] with the enantioseparation factor $\alpha = 1.08$ (40 °C). In order to examine the possible diastereomerization of **2a**, a stopped-flow experiment[23] was performed as follows. The flow of the carrier gas was switched off exactly at the time when both (already separated) enantiomers were located in the centre of the gas-chromatographic capillary. The temperature of the oven was quickly increased up to 190 °C and kept for 10 min followed by fast cooling to 40 °C and proceeding with the separation at 50 kPa of the carrier gas pressure.

Crystal data: The crystallographic data have been deposited with the Cambridge Crystallographic Data Center, CCDC 255386 for **2a**·picrate, CCDC 255387 for **2b**·HCl and CCDC 255388 for **7**. Copies of this information may be obtained free of charge from: The Director, CCDC, 12 Union Road, Cambridge, CB2 1EZ, UK (fax: +44-1223-336033; e-mail: deposit@ccdc.cam.ac.uk or http://www.ccdc.cam.ac.uk).

Acknowledgements

This work was supported by the Russian Foundation for Basic Research (Grant No. 06-03-32840), and the Russian Academy of Sciences. P. Levkin thanks the Graduate College 'Chemistry in Interphases' for the financial support.

References

1. Lenev, D. A.; Chervin, I. I.; Lyssenko, K. A.; Kostyanovsky, R. G. *Tetrahedron Lett.* **2007**, *48*, 3363.
2. Kostyanovsky, R. G.; Korneev, V. A.; Chervin, I. I.; Voznesensky, V. N.; Puzanov, Yu. V.; Rademacher, P. *Mendeleev Commun.* **1996**, 106.
3. Makhova, N. N.; Kuznetsov, V. V.; Kostyanovsky, R. G. *Izv. Akad. Nauk. Ser. Khim.* **1996**, 1870 (in Russian).
4. Trapp, O.; Schurig, V.; Kostyanovsky, R. G. *Chem. Eur. J.* **2004**, *10*, 951.
5. Kostyanovsky, R. G.; Kadorkina, G. K.; Voznesensky, V. N.; Chervin, I. I.; Antipin, M. Yu.; Lyssenko, K. A.; Vorontzov, E. V.; Bakhmutov, V. I.; Rademacher, P. *Mendeleev Commun.* **1996**, 69.
6. Kostyanovsky, R. G.; Rademacher, P.; El'natanov, Yu. I.; Kadorkina, G. K.; Nikiforov, G. A.; Chervin, I. I.; Usachev, S. V.; Kostyanovsky, V. R. *Russ. Chem. Bull.* **1997**, *46*, 1291.
7. Baker, V. J.; Katritzky, A. R.; Majoral, J.-P. *J. Chem. Soc., Perkin Trans.* **1975**, 1191.
8. Baker, V. J.; Katritzky, A. R.; Majoral, J.-P.; Nelsen, S. F.; Hintz, R. J. *J. Chem. Soc., Chem. Commun.* **1974**, 823.
9. Kostyanovsky, R. G.; Kadorkina, G. K.; Kostyanovsky, V. R.; Schurig, V.; Trapp, O. *Angew. Chem., Int. Ed.* **2000**, *39*, 2938.
10. Usachev, S. V.; Nikiforov, G. A.; Strelenko, Yu. A.; Belyakov, P. A.; Chervin, I. I.; Kostyanovsky, R. G. *Mendeleev Commun.* **2002**, 189.
11. Usachev, S. V.; Nikiforov, G. A.; Strelenko, Y. A.; Chervin, I. I.; Lyssenko, K. A.; Kostyanovsky, R. G. *Mendeleev Commun.* **2003**, 136.
12. Lehn, J.-M. *Fortschr. Chem. Forsch* **1970**, *15*, 311.
13. Lehn, J.-M.; Wagner, J. *Tetrahedron* **1970**, *26*, 4227 (Dietrich, B.; Lehn, J.-M.; Linscheid, P., unpublished results).
14. Ioffe, B. V.; Kuznetsov, M. A.; Potekhin, A. A. *Chemistry of organic derivatives of hydrazines*; Khimia: Leningrad, 1979; pp 79–86 (in Russian).
15. *Enamines: Synthesis, Structure, and Reactions*; Gilbert Cook, A., Ed.; Marcel Dekker: New York and London, 1969; pp 162–164.
16. Coulter, J. M.; Lewis, J. W.; Lynch, P. P. *Tetrahedron* **1968**, *24*, 4489.
17. de Benneville, P. L.; Macartney, J. H. *J. Am. Chem. Soc.* **1950**, *72*, 3073.
18. Mintas, M.; Mannschreck, A.; Klasing, L. *Tetrahedron* **1981**, *37*, 867.
19. Wilen, S. H.; Qi, J. Z.; Williard, P. G. *J. Org. Chem.* **1991**, *56*, 485.
20. Ioffe, B. V.; Poroshin, L. E. *Zhur. Obscch. Khim.* **1959**, *8*, 3154.
21. Schurig, V.; Schmalzing, D.; Muehleck, U.; Jung, M.; Schleimer, M.; Mussche, P.; Duvekot, C.; Buyten, J. C. *J. High Res. Chromatogr.* **1990**, *13*, 713–717.
22. Cousin, H.; Trapp, O.; Peulon-Agasse, V.; Pannecoucke, X.; Banspach, L.; Trapp, G.; Jiang, Z.; Combret, J. C.; Schurig, V. *Eur. J. Org. Chem.* **2003**, *17*, 3273–3287.
23. Wolf, C. *Chem. Soc. Rev.* **2005**, *34*, 595–608.
24. Nelubina, Y. V.; Lyssenko, K. A.; Kravchenko, A. N.; Antipin, M. Yu.; Sigachev, A. S. *Russ. Chem. Bull.* **2006**, *3*, 387–395 (*Izv. Akad. Nauk., Ser. Khim.* **2006**, *3*, 387–396, in Russian).